15.1 The maintenance of tornadoes observed with high-resolution mobile radars

JAMES MARQUIS*, YVETTE RICHARDSON, AND PAUL MARKOWSKI

Department of Meteorology, Pennsylvania State University, University Park, PA

JOSHUA WURMAN

Center for Severe Weather Research, Boulder, CO

DAVID DOWELL

National Center for Atmospheric Research, Boulder, CO

1. Introduction

There are several unsolved fundamental aspects of the tornado problem. One of these aspects is the uncertainty as to how kinematic traits of the storm and mesoscale environment influence tornado longevity. Whereas a few studies (e.g. Wicker and Wilhelmson 1995; Xue 2004) have discussed the maintenance of particular mature tornadoes by analyzing the dynamic/kinematic aspects of the nearby airflow, no analysis across many observed storms exists. A knowledge of the factors influencing tornado longevity has obvious forecasting implications, such as determining which storms are likely to support long-lasting tornadoes.

This study employs single and dual-Doppler mobile radar observations collected in several supercell thunderstorms in order to determine the mesoscale and storm-scale kinematic features that are responsible for maintaining tornadoes and the processes that cause their disruption. For example, we seek to test the hypothesis formulated by Dowell and Bluestein (2002b) that the maintenance of tornadoes is related to their position relative to the primary updraft. While the examination of this and other relevant hypotheses is still ongoing, the preliminary results indicate that storm-relative advection of the vertical vorticity field causes some of the tornadoes to change their motion near the time of dissipation, possibly consistent with the results of Dowell and Bluestein (2002b). Many tornadoes appear to decay in outflow air that has fully surrounded the low-level mesocyclone.

2. Method

High-resolution Doppler radar data collected by two Doppler on Wheels radars (Wurman et al. 1997) during the Radar Observations of Tornadoes and Thunderstorms Experiment (ROTATE 1998 – 2006) are analyzed in four tornadic supercell storms. Dual-Doppler wind syntheses are available for limited times in most data sets. Objective analysis is performed using an isotropic Barnes weighting function with the smoothing parameters chosen such that, when quantitatively comparing common features in multiple data sets, all data sets are smoothed equally, based on the largest azimuthal spacing observed out of all of the cases. Otherwise, smoothing is case dependent, and is based on the largest azimuthal spacing observed in the desired domain of each data set. The position of the objectively analyzed data is corrected to a central time in each volume using the horizontal motion of the tornado. The 3-D wind field is obtained by an upward integration of the anelastic mass continuity equation with $w = 0$ at the lower boundary. An iterative technique was used to adjust the u, v, and w fields until the change in density-weighted w was less than 0.01 kg m^{-2} s^{-1}. Single-Doppler data are used when dual-Doppler data are not available.

*Corresponding author address: James Marquis, Department of Meteorology, Pennsylvania State University, 503 Walker Building, University Park, PA 16802; *e-mail*: jmarquis@met.psu.edu.

3. Observations

Figure 1 shows the intensity (in terms of the estimated axisymetric tangential velocity, V_t, determined by taking one half the differential of peak inbound and outbound radial velocity observed in unsmoothed single-Doppler data from the nearest radar) versus time for the tornadoes examined so far in this study. The full lifecycle of some of the long-duration tornadoes analyzed herein is not observed by the radars; hence, the lifetimes of these tornadoes are determined using visual evidence (video and still photographs) and a NOAA-NCDC database of tornado events. The DOW radars collected data in at least two long-lived tornadoes (4 June 1999 and 15 May 2003, both lasting longer than 20 minutes) at times when their intensity transitions from a nearly steady state to a permanent state of weakening. We also examine a few short-lived tornadoes (e.g. 5 June 2001 and 30 April 2000, both lasting less than 8 minutes), where an initial intensification to tornadic intensity is soon followed by a state of steady and rapid weakening. As a first step in understanding tornado longevity, we will examine these transitions from steady or increasing intensity to dissipation to see which storm-scale processes are associated with such a change.

a. Tornado decay

Qualitatively, it often appears that the transition to a permanent weakening trend occurs when the initial occlusion of outflow air associated with tornadogenesis (e.g. Brandes 1977; Brandes 1978; Lemon and Doswell 1979) progesses such that outflow air prevents contact between the low-reflectivity, presumably

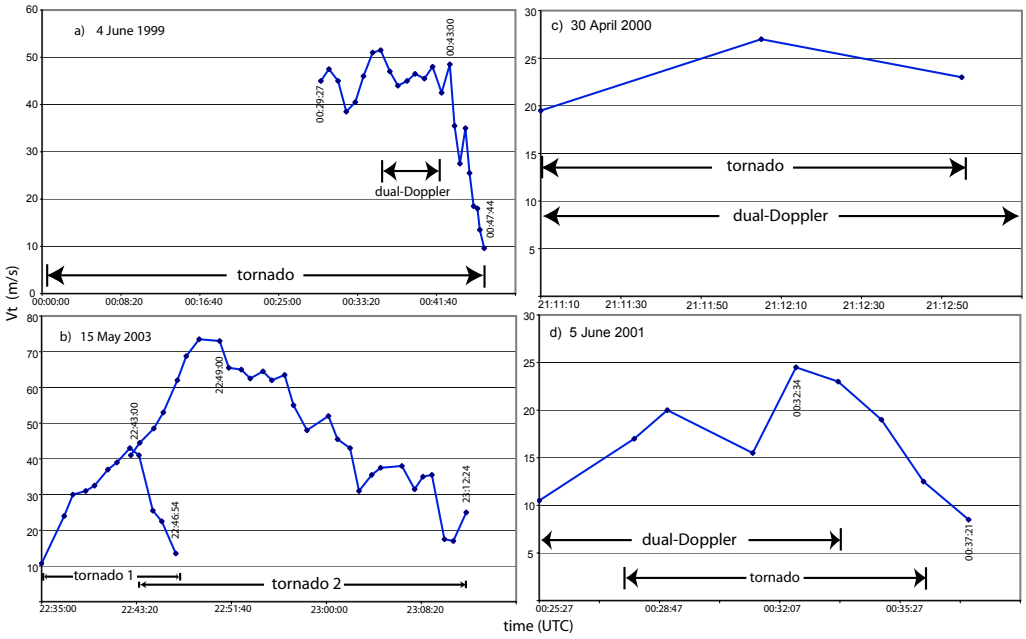

FIG. 1. Estimated axisymmetric tangential velocity (V_t) versus time (UTC) in 5 tornadoes observed by the DOWs. Two tornadoes are observed on 15 May 2003 (b). Times when dual-Doppler data are available are indicated in each panel; at other times only single-Doppler data are available.

buoyant, inflow air and the tornado. This progressive occlusion process is consistent with the presence of negatively buoyant air wrapping around the entire mesocyclone at low-levels, which causes the decay of the primary storm updraft, mesocyclone, and tornado in many observed and simulated supercells (e.g. Wicker and Wilhelmson 1995; Wurman et al. 2006).

Dowell and Bluestein (2002a,b), however, describe a process whereby the tornado moves relative to the main storm updraft, due to updraft-relative advection of vertical vorticity, and loses its intensity. Indeed, the motion of the tornadic circulation on 5 June 2001 (shown in Fig. 2) appears to be dictated by the horizontal advection of vertical vorticity. The horizontal advection term in the vertical vorticity equation dominates over both the tilting and stretching terms at low-levels (also shown in Fig. 2), and the motion of the center of circulation approximately follows the maximum value of advection at each time. Throughout Fig. 2, the north-south component of motion of the vertical vorticity maximum changes from due north to due south, then back to due north. During this sequence, changes in the character of outflow winds occur that change the position of the horizontal advection maximum relative to the vertical vorticity maximum. For example, strong northwesterly outflow just west and southwest of the center of rotation at 002933 UTC (Fig. 2b) has maximized horizontal advection south and southeast of the tornado, causing it to deviate from its northeastward motion. The strong northwesterly winds weaken a bit by 003416 UTC (Fig. 2c), and s ‘trong southwesterly winds are evident just east of the tornado as some of the surging outflow wraps around it. The tornado, which is beginning to weaken, is advected to the east-northeast just before it exits the dual-Doppler domain. Also at this time, the center of rotation is collocated with weak divergence, suggesting that this causes its eventual dissipation a few minutes later. This observation of tornado motion appears to be consistent with the findings of Dowell and Bluestein (2002b). However, in their study, the tornadoes were advected rearward into the outflow while the updraft continued. In our case, dual-Doppler data do not extend sufficiently forward in time to establish this relationship between the tornado motion and the updraft motion.

The observation that the outflow behind the rear-flank gust front (hereafter RFGF) wraps around the dissipating tornado is not observed in every storm. At the approximate time when a long-lived tornado on 4 June 1999 begins to steadily and significantly decay ($\sim$ 0043 UTC), the tornado is in very close proximity to the RFGF and is located near the inflow air. Approximately two minutes before this time, a region of strong storm inflow exists ahead of the RFGF and in close proximity to the tornado (Fig. 3b). The RFGF is no longer circling around the tornado and mesocyclone, but rather, is approximately north-south oriented indicating a retreat of the RFGF with respect to the tornado. The reorientation of the RFGF is consistent with a change in the relative magnitude of low-level outflow and inflow across the RFGF. The motion of the tornado (also shown in Fig. 3), which changes from toward the northeast to toward the northwest after this time, causes it to migrate toward the precipitation swath associated with the hook echo of the storm where it dissipates. This deviation of the tornado motion just to prior its weakening and eventual dissipation also appears to be

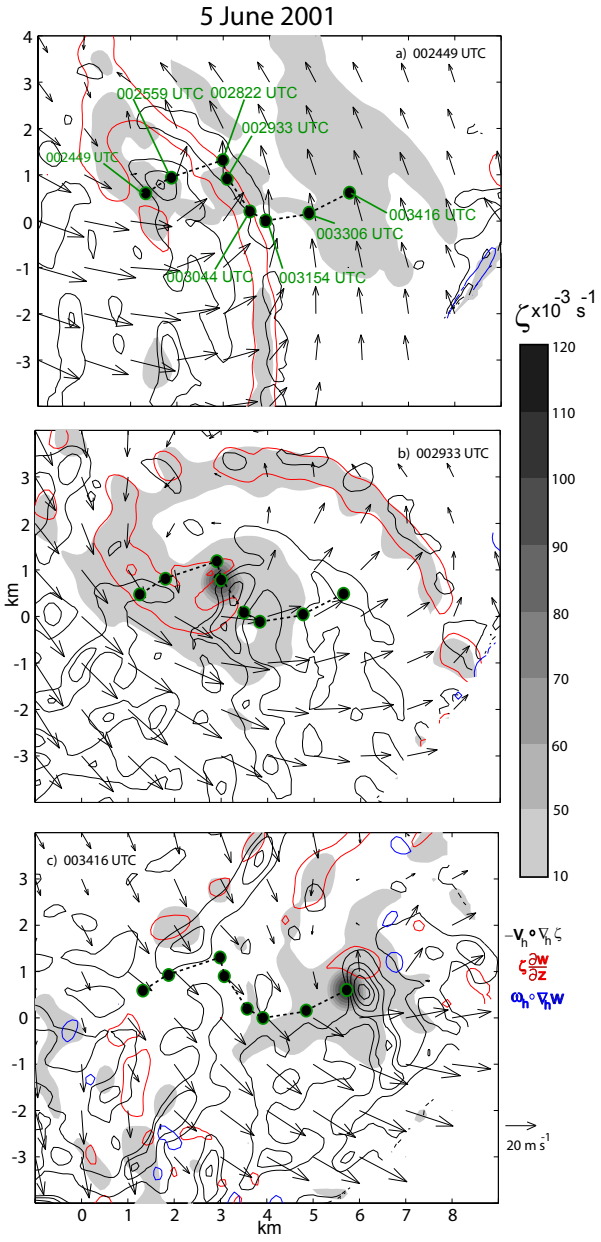

FIG. 2. Vertical vorticity (shaded), vertical tilting of horizontal vorticity (blue contours), vertical stretching of vertical vorticity (red contours), horizontal advection of vertical vorticity (black contours), and ground-relative wind (vectors) at z = 300 m AGL at 002449 UTC (a), 002933 UTC (b), and 003416 UTC (c) on 5 June 2001. The first (outermost) contours of tilting, stretching and advection are .001 s^{-2}, incremented by 0.005 s^{-2}. The position of the tornado is shown in all images as circles at the times shown in (a).

consistent with Dowell and Bluestein (2002b). Unfortunately, dual-Doppler data is not available at the time of dissipation on 4 June 1999 to determine exactly where the vertical vorticity supplying the tornado originates and to determine the position of the tornado relative to the storm updraft.

b. Nontornadic vertical vorticity maxima

In some of the cases, small ($\sim$ 0.5 – 1.0 km diameter) vertical vorticity maxima ($10^{-3}\ s^{-1} < \zeta < 10^{-1}\ s^{-1}$) are observed along the RFGF. For example, on 5 June 2001 several positive vertical vorticity maxima below 300 m AGL spiral inward toward the center of mesoscale rotation (Fig. 4). It is of future interest to this study to determine if these vorticity maxima play a role in maintaining an existing tornado. Negative vertical vorticity maxima are also present along some RFGFs, and in some cases, both positive and negative maxima are present. This observation, along with the fact that not all tornadoes exist at times when other vertical vorticity maxima are located along the RFGF (e.g. the long-lived 4 June 1999 tornado), suggests that if they do play a role in maintaining tornadoes, they may only be significant in some storms.

4. Summary and future work

Mobile Doppler radar data are examined in several tornadic supercell storms to determine what factors influence the dissipation of tornadoes. In most cases it is found that the tornadoes begin to dissipate when outflow air wraps around them and cuts off low-level inflow to the updraft. The storm-relative position of the tornado appears to be influenced by trends in the strength of storm-relative inflow or outflow, and some of the dissipating tornadoes deviate from their previous motions when they begin to weaken. This observation might be consistent with some of the findings of Dowell and Bluestein (2002), as is the relative significance of horizontal advection to the other terms in the vertial vorticity equation at low levels.

As this study progresses, we hope to retrieve the 3-D wind field in single-Doppler cases as well. If successful, we will be able to locate source regions of vertical vorticity that supply the tornado over a greater portion of its lifetime than that observed by dual-Doppler and determine what common storm-scale features later disrupt these source regions or prevent trajectories from passing through them for a sufficiently long time to acquire tornadic intensity. Additionally, the retrieved data will allow us to test the hypothesis that the updraft-relative position of the tornado is also a relevant factor in maintaining the tornado at times when dual-Doppler data are not available for such confirmation. We also hope to retrieve thermodynamic fields in each storm in order to assess the buoyancy of parcels passing through the tornadoes.

Acknowledgments. The authors would like to thank Curtis Alexander for his assistance with dorade processing codes and data support, and Nettie Arnott for allowing us to use her wind synthesis and objective analysis scripts. We also thank Herb Stein, Bob Conzemius, and Charles Edwards for their storm video of certain cases and the crew of the DOW radars on the days analyzed herein. Radar data editing, objective analysis, and wind syntheses were performed and viewed using Solo II, REORDER, CEDRIC, and Vis5d. We thank the writers of these programs. This project is funded by NSF grants ATM-0437512, 0437505, and 0437898.

REFERENCES

Barnes, S. L., 1964: A technique for maximizing details in numerical weather map analysis. *J. Appl. Meteor.*, **3**, 396–409.

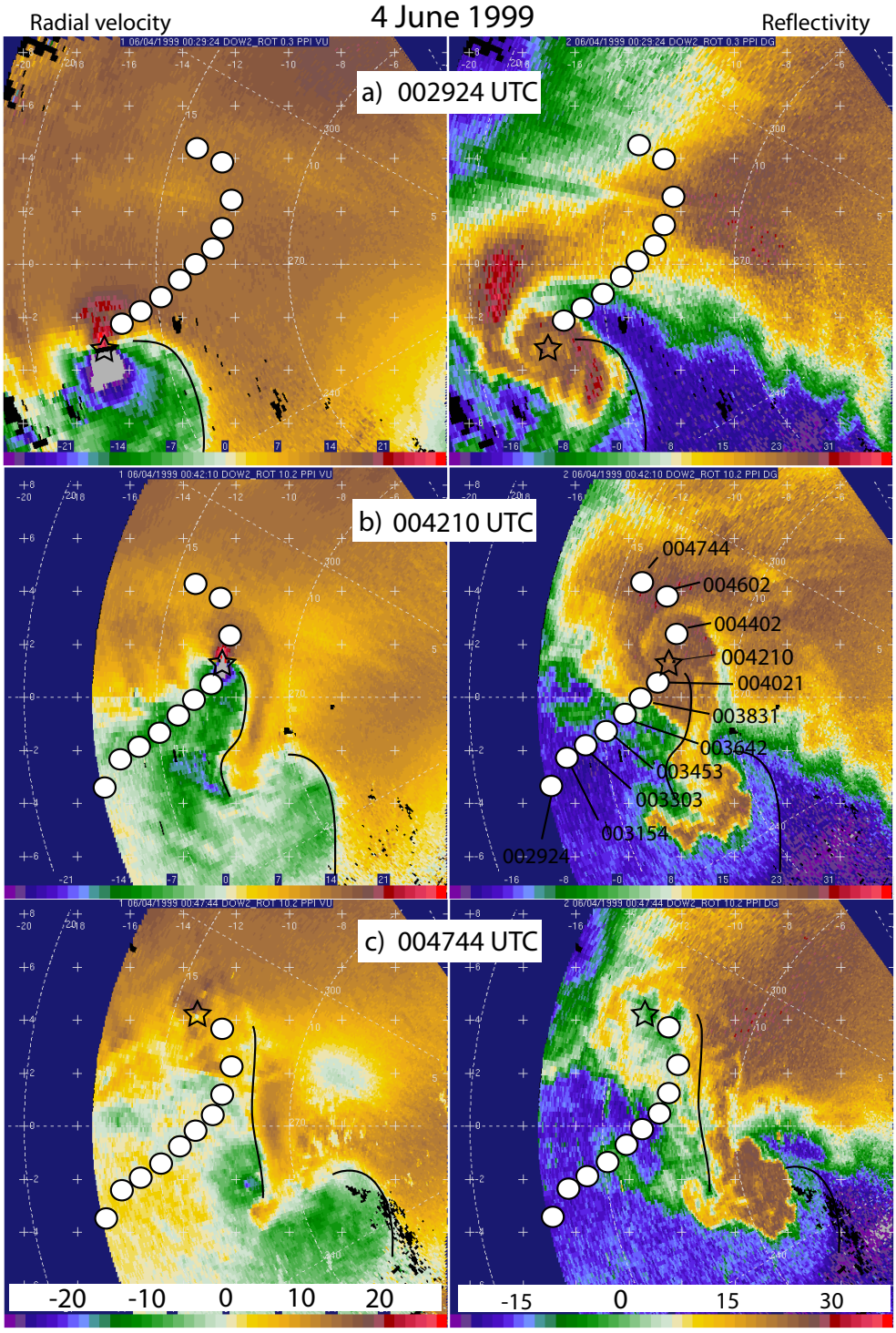

FIG. 3. Radial velocity data (m s^{-1}, left) and radar reflectivity factor (right) in the 0.5° elevation sweep from DOW 2 on 4 June 1999 between 002924 UTC (a) and 004744 UTC (c). The position of the tornado is shown in all images as circles (and stars for the time represented in each particular panel), the times for each position are shown in b) on the right. The approximate location of the rear-flank gust front is indicated in each image with a black line. White tick marks are shown every 2 km.

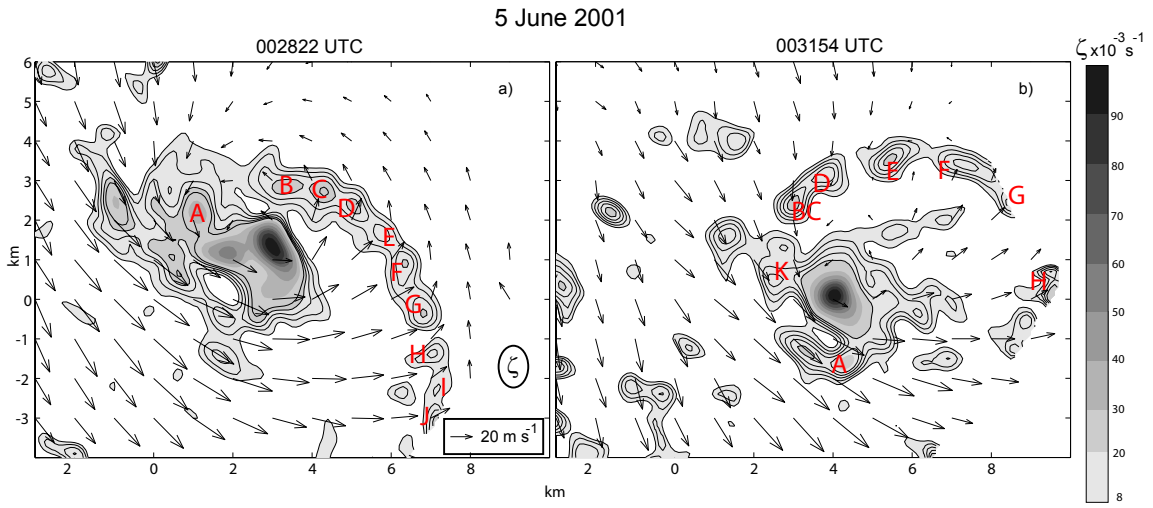

FIG. 4. Vertical vorticity from 0.008 s^{-1} to 0.02 s^{-1} in increments of 0.003 s^{-1} (contoured) and ground-relative wind (vectors) at z = 300 m AGL at 002822 UTC (a) and 003154 UTC (b) on 5 June 2001. Vertical vorticity is also shaded. Individual vorticity maxima are labeled by letter to assist tracking them. 'BC' indicates that 'B' and 'C' have merged. 'K' is a new vorticity maxima that forms between 002822 and 003154.

Brooks, H.E., 2004: On the relationship of tornado path length and width to intensity. *Wea. Forecasting*, **19**, 310–319.

Brandes, E.A., 1977: Gust front evolution and tornado genesis as viewed by Doppler radar. *J. Appl. Meteor.*, **16**, 333–338.

Brandes, E.A., 1978: Mesocyclone evolution and tornadogenesis: some observations. *Mon. Wea. Rev.*, **106**, 995–1011.

Dowell, D.C, 2002: Observations of the formation of low-level rotation: The 5 June 2001 Sumner County, Kansas storm. *21st Conf. on Severe Local Storms*, San Antonic, TX, Amer. Meteor. Soc.

Dowell, D. C., and H. B. Bluestein, 2002a: The 8 June 1995 McLean, Texas storm. Part I: Observations of cyclic tornadogenesis. *Mon. Wea. Rev.*, **130**, 2626–2648.

Dowell, D. C., and H. B. Bluestein, 2002b: The 8 June 1995 McLean, Texas storm. Part II: Cyclic tornado formation, maintenance, and dissipation. *Mon. Wea. Rev.*, **130**, 2649–2670.

Klemp, J. B., R. B. Wilhelmson, and P. S. Ray, 1981: Observed and numerically simulated structure of a mature supercell thunderstorm. *J. Atmos. Sci.*, **38**, 1558–1580.

Lee, B.D., and R. B. Wilhelmson, 1997: The numerical simulation of non-supercell tornadogenesis. Part II: Evolution of a family of tornadoes along a weak outflow boundary. *J. Atmos. Sci.*, **54**, 2387–2414.

Pauley, P. M., and X. Wu, 1995: The theoretical, discrete, and actual response of the Barnes objective analysis scheme for one- and two-dimensional fields. *Mon. Wea. Rev.*, **118**, 1145–1163.

Rotunno, R., and J. Klemp, 1985: On the rotation and propagation of simulated supercell thunderstorms. *J. Atmos. Sci.*, **42**, 271–292.

Trapp, R. J.,and C. A. Doswell, 2000: Radar objective analysis. *J. Atmos. Oceanic Tech.*, **117**, 105–120.

Wicker, L.J., and R.B. Wilhelmson, 1995: Simulation and analysis of tornado development and decay within a three-dimensional supercell thunderstorm. *J. Atmos. Sci.*, **52**, 2675–2703.

Wicker, L.J., 1996: The role of near surface wind shear on low-level mesocyclone generation and tornadoes. *18th Conf. on Severe Local Storms*, San Francisco, CA, Amer. Meteor. Soc.

Wurman, J., J.M. Straka, M. Randall and A. Zahrai, 1997: Design and development of a portable, pencil-beam, pulsed, 3-cm Doppler radar. *J. Atmos. Oceanic Tech.*, **14**, 1502–1512.

Wurman, J, 2002: Observations of the formation of low-level rotation: The 5 June 2001 Sumner County, Kansas storm. *21st Conf. on Severe Local Storms*, San Antonic, TX, Amer. Meteor. Soc.

Wurman, J., Y. Richardson, C. Alexander, S. Weygandt, and P. Zhang, 2006: Dual-Doppler analysis of winds and vorticity budget terms near a tornado., *Submitted to Mon. Wea. Rev.*

Xue, M., 2004: Tornadogenesis within a simulated supercell storm. Preprints, *22nd Conf. on Severe Local Storms,* Hyannis, MA, Amer. Meteor. Soc.